Applied Ergonomics 109 (2023) 103981

Contents lists available at ScienceDirect

Applied Ergonomics

journal homepage: www.elsevier.com/locate/apergo

# Gyroscope vector magnitude: A proposed method for measuring angular velocities

Howard Chen[a,b,*], Mark C. Schall[c], Nathan B. Fethke[d]

[a] Industrial & Systems Engineering and Engineering Management Department, The University of Alabama in Huntsville, Huntsville, AL, USA
[b] Department of Mechanical Engineering, Auburn University, Auburn, AL, USA
[c] Department of Industrial & Systems Engineering, Auburn University, Auburn, AL, USA
[d] Department of Occupational & Environmental Health, The University of Iowa, Iowa City, IA, USA

ABSTRACT

High movement velocities are among the primary risk factors for work-related musculoskeletal disorders (MSDs). Ergonomists have commonly used two methods to calculate angular movement velocities of the upper arms using inertial measurement units (accelerometers and gyroscopes). Generalized velocity is the speed of movement traveled on the unit sphere per unit time. Inclination velocity is the derivative of the postural inclination angle relative to gravity with respect to time. Neither method captures the full extent of upper arm angular velocity. We propose a new method, the gyroscope vector magnitude (GVM), and demonstrate how GVM captures angular velocities around all motion axes and more accurately represents the true angular velocities of the upper arm. We use optical motion capture data to demonstrate that the previous methods for calculating angular velocities capture 89% and 77% relative to our proposed method.

## 1. Introduction

Inertial measurement units (IMUs) can quantify occupational risk factors for musculoskeletal disorders (MSDs), such as high movement velocities (Arvidsson et al., 2021; Kersten and Fethke, 2019; Schall et al., 2021). An IMU contains triaxial gyroscopes, accelerometers, and magnetometers, which allows a variety of approaches to kinematic measurements such as full-body inertial motion capture (Robert-Lachaine et al., 2019), inclinometry using gyroscope and accelerometer measurements (IMU-based inclinometer) (Chen et al., 2020; Fan et al., 2021; Schall et al., 2021), and inclinometry using accelerometer measurements (accelerometer-based inclinometer) (Chen et al., 2018). In contrast to full-body inertial motion capture, IMU-based inclinometers are not susceptible to errors from gyroscopic drift or ambient magnetic field disturbances (Chen et al., 2020; Schall Jr. et al., 2016b). However, the primary limitation of IMU-based inclinometers is an inability to measure movement around the gravity vector.

The angular velocities of body segments, particularly the upper arm, have been frequently quantified with inclinometers (Douphrate et al., 2012; Granzow et al., 2018; Schall Jr. et al., 2016a; Veiersted et al., 2008) using one of two computational methods: inclination velocity (Douphrate et al., 2012; Granzow et al., 2018; Schall et al., 2021) or generalized velocity (Arvidsson et al., 2012; Balogh et al., 2019; Veiersted et al., 2008). Inclination velocity is obtained by derivation of upper arm inclination angle (relative to gravity) with respect to time. Generalized velocity is defined as the distance traveled on the unit sphere per time unit (Hansson et al., 2001) and, in general, produces higher velocity magnitudes than inclination velocity because rotations in multiple directions are factored in the calculation (Fan et al., 2021). Differences in measurements between the inclination and generalized velocity approaches have been highlighted (Fan et al., 2021; Forsman et al., 2022a) and are important given recently proposed occupational exposure thresholds for movement velocities (Arvidsson et al., 2021). Inclination and generalized velocity can be calculated using accelerometer data alone, for which motion introduces measurement error (Chen et al., 2018), or in combination with gyroscope data and a sensor fusion algorithm (Fan et al., 2021), which reduces measurement error but increases computational overhead. Forsman et al. (2020b) proposed conversion models to resolve differences between accelerometer and IMU-derived upper arm inclination velocities and generalized velocities. They indicated that more studies are needed to determine one common standard metric for reporting upper arm angular velocities. One motivating factor is that neither inclination velocity nor generalized velocity capture angular velocity in all movement directions.

Few studies have evaluated the accuracy of accelerometer and IMU-derived angular velocity measurements or their associated movement

* Corresponding author. Industrial & Systems Engineering and Engineering Management Department, The University of Alabama in Huntsville, Huntsville, AL, USA.

E-mail address: howard.chen@uah.edu (H. Chen).

https://doi.org/10.1016/j.apergo.2023.103981
Received 12 September 2022; Received in revised form 7 December 2022; Accepted 18 January 2023
Available online 3 February 2023

summary measures used for health-based decision-making in the context of occupational ergonomics (Chen et al., 2020, 2018; Schall Jr. et al., 2016b, 2015; Yang et al., 2017). We reported a root-mean-square (RMS) error of 79°/s for accelerometer-derived upper arm inclination velocity for 'fast' motion during a cyclic material handling task (45 cycles/min), using optical motion capture (OMC) as a reference (Chen et al., 2018). An important observation from that study was the underestimation of the extreme upper arm postures and velocities (i.e., 90th percentiles) at increased motion speeds. Such underestimation may impact observed associations between summary measures of exposure and musculoskeletal health outcomes in epidemiologic studies. Fan et al. (2021) observed an average difference of 50°/s between accelerometer- and IMU-derived generalized velocities, despite mean differences <2° in inclination angles. Notably, they observed that accelerometer-derived upper arm generalized velocities were 100°/s greater than the IMU-derived upper arm generalized velocities for the 90th and 99th percentile summary measures. Similarly, Yang et al. (2017) reported mean absolute differences of 300°/s and 452°/s in the 90th percentile of accelerometer-derived inclination and generalized velocities, respectively, in comparison to OMC. Consistent with Chen et al. (2020), the results of Yang et al. (2017) suggested (i) a clear increase in mean absolute differences as motion speed increased and (ii) a substantial reduction in mean absolute difference in comparison to OMC when combining accelerometer and gyroscope data to calculate angular velocity (either inclination or generalized). However, their associated movement summary measures used to quantify exposure to high movement velocities were not provided.

Because of the availability of gyroscope data from an IMU, it seems counterintuitive to rely on accelerometer data in addition to gyroscope data when calculating upper arm angular velocity. The gyroscope vector magnitude incorporates rotation in all movement directions, in contrast to inclination and generalized velocity, and does not impose a computational penalty of using a sensor fusion algorithm. The gyroscope vector magnitudes from wrist- and hip-worn IMUs have been used to estimate energy expenditure during activities of daily living (Hibbing et al., 2018; Marcotte et al., 2018). In an ergonomics context, Manivasagam and Yang (2022) reported the difference in gyroscope vector magnitudes from IMUs positioned on the hand and forearm as a measure of "total" wrist angular velocity (vs. velocity obtained through differentiation of data from a standard biaxial electrogoniometer). However, Manivasagam and Yang (2022) did not provide a biomechanical definition for this quantity, which is necessary for researchers and practitioners to interpret its meaning.

In this paper, we expand on (i) the work of Fan et al. (2021) and Yang et al. (2017) by evaluating the accuracy of accelerometer and IMU-derived generalized velocity measurements for the upper arm and their associated summary metrics, and (ii) expand on the work of Manivasagam and Yang (2022) by providing a biomechanical definition of gyroscope vector magnitude necessary for its use as an exposure measure in occupational ergonomics applications. We also use OMC measurements to demonstrate how gyroscope vector magnitude captures angular velocity to a fuller extent than both inclination and generalized velocity.

## 2. Methods

### 2.1. Angular velocity calculation methods

#### 2.1.1. Inclination velocity

We define inclination velocity as the absolute value of the rate of change of upper arm elevation angle (relative to gravity) with respect to time. Inclination velocity (incVel) can be calculated as follows:

$$\dot{\theta}_k = \frac{|\theta_k - \theta_{k-1}|}{\Delta t} \tag{1}$$

where $\theta_k$ and $\theta_{k-1}$ are the upper arm elevation angles relative to gravity at instance $k$ and $k-1$, respectively, and $\Delta t$ is the sampling period.

Upper arm elevation is calculated as follows:

$$\theta_k = \cos^{-1}\left(-g_{x,k}\right) \tag{2}$$

where $g_{x,k}$ is the x-component of the normalized gravitational vector in the sensor frame. Note that $\vec{g}_k$ is in the sensor frame. Therefore, this value will change with sensor inclination. $\vec{g}_k$ can therefore be thought of as the normalized accelerometer measurements in the absence of non-gravitational acceleration. Since $\vec{g}_k$ can be decomposed into 'pitch' and roll' angles (Pedley, 2013), $\vec{g}_k$ can also be considered as the combination of 'pitch' and 'roll' angles. Equation (2) assumes that the x-axis of the IMU is aligned with the upper arm, with positive x oriented distally. While this method is easily interpretable, incVel does not change when the upper arm is moved purely around gravity, i.e., upper arm movements with no change in elevation angle.

#### 2.1.2. Generalized velocity

Generalized velocity has been defined as the angle traveled on the unit sphere per time unit (Fan et al., 2021). Detailed explanations of generalized velocities can be found elsewhere (Fan et al., 2021; Hansson et al., 2001, 2006). In contrast to incVel, this approach considers two movement directions, capturing angular velocities to a fuller extent than incVel.

Generalized velocity can be calculated as follows (Fan et al., 2021):

$$\mathrm{VDGV} = \frac{2\ \mathrm{asin}\left(\frac{\left\|\vec{g}_k - \vec{g}_{k-1}\right\|_2}{2}\right)}{\Delta \mathrm{t}} \tag{3}$$

where $\vec{g}_{k-1}$ and $\vec{g}_k$ are the normalized gravitational vectors in the sensor frame at instances k-1 and k, respectively. Since this method requires differencing the gravitational vectors, we will refer to this calculation method as vector-differenced generalized velocity (VDGV).

The primary difference between incVel and VDGV is that VDGV considers arm internal/external rotation in addition to inclination velocity (Forsman et al., 2022b). Specifically, pure inclination velocity will register the same value for both incVel and VDGV. Pure internal/external motion will register on VDGV but not incVel. Pure plane of elevation motion will theoretically register on neither.

The angle ($\beta$) between two unit vectors can be calculated by taking the arc-cosine of the dot product. Given $\vec{g}_{k-1}$ and $\vec{g}_k$, $\beta$ can also be conceptualized as the net angular change between successive unit vectors (*4*). Therefore, dividing $\beta$ by the sample period yields the rate of angular change between successive directional unit vectors, or the angular velocity ($\dot{\beta}$) (*5*). This provides the same quantity as (*3*).

VDGV can, therefore, be alternatively calculated as follows:

$$\beta = \mathrm{acos}\left(\vec{g}_{k-1} \bullet \vec{g}_k\right) \tag{4}$$

$$\dot{\beta} = \mathrm{VDGV} = \frac{\beta}{\Delta \mathrm{t}} \tag{5}$$

where $\bullet$ is the vector dot product.

There are two fundamental limitations to using incVel or VDGV for quantifying angular velocities. First, when $\vec{g}$ is derived from accelerometer data alone, the accuracy of incVel is adversely affected by non-gravitational acceleration, particularly during high-speed movements (Bernmark and Wiktorin, 2002; Chen et al., 2020; Yang et al., 2017). The measurement accuracy of incVel can be improved, however, by combining accelerometer and gyroscope measurements with a sensor fusion algorithm (e.g., Kalman filter or complementary filter) (Chen et al., 2018, 2020; Johnson et al., 2022; Ligorio and Sabatini, 2015). Second, neither incVel nor VDGV incorporates rotations around gravity;

therefore, neither method captures the full extent of angular velocity.

#### 2.1.3. Gyroscope vector magnitude

We propose using the gyroscope vector magnitude (GVM) to quantify movement velocities rather than incVel or VDGV. GVM can capture angular velocity around all movement directions since obtaining $\vec{\omega}$ by differencing orientation measurements will present no further loss of information beyond its initial orientation. This can be verified by calculating $\vec{\omega}$ by differencing orientation measurements and subsequently re-calculating orientation using $\vec{\omega}$, $\Delta t$, and an initial orientation (Appendix B). The result will match the original set of orientation measurements.

GVM is calculated as follows:

$$\mathrm{GVM} = \|\vec{\omega}\|_2 = \sqrt{\omega_x^2 + \omega_y^2 + \omega_z^2} \tag{6}$$

where $\omega_x$, $\omega_y$, and $\omega_z$ are the angular velocity measurements around the sensor x, y, and z-axes. The vector magnitude of $\vec{\omega}$ is defined as the rate of directional change between successive coordinate frames, and a mathematical derivation is shown in Appendix B. While $\vec{\omega}$ is most easily obtained directly from gyroscope measurements, it can also be obtained by differencing orientation measurements (See Appendix C). This calculation assumes that humans typically take the shortest path between two positions.

### 2.2. Experimental method

#### 2.2.1. Participants and experimental task

This study used data collected for a laboratory evaluation of IMUs among 13 right-handed participants (11 male; mean age = 27.2 ± 6.6 years). We refer to previous studies for detailed protocols and instrumentation (Chen et al., 2017, 2018, 2020). Briefly, exclusion criteria included any self-reported cases of (i) physician-diagnosed MSD in the previous six months, (ii) pain during the two weeks prior to study enrollment, and (iii) history of orthopedic surgery in the upper extremity (shoulder, elbow, wrist, hand). Written informed consent was obtained prior to data collection. The study protocol was approved by the University of Iowa Institutional Review Board.

Participants completed six 1-min trials of a repetitive reaching task that required transferring wooden dowels (2 cm diameter x 8 cm length) from a container placed directly in front of each participant's waist to a container placed approximately 45° offset diagonally from the participant at shoulder level. Participants completed two trials at each of three transfer rates dictated by a metronome: slow (15 cycles/min), medium (30 cycles/min), and fast (45 cycles/min). Experimental conditions were randomized to control for potential order effects. Participants were acclimated to the assigned transfer rate before recording OMC measurements for each trial, followed by a 5-min rest period. This experiment used the material transfer rate as a proxy for movement speed.

#### 2.2.2. Instrumentation

Participants were fitted with an IMU on the lateral aspect of the dominant upper arm midway between the acromion and the lateral epicondyle (Opal, APDM, Inc. Portland, OR; also sold as series SXT, Nexgen Ergonomics, Inc., Pointe Claire, Quebec, CA). The IMU was secured using Velcro® straps. Raw accelerometer and gyroscope measurements were sampled from the IMUs at 128 Hz. A six-camera OMC system (Optitrack Flex 13, NaturalPoint, Inc., Corvallis, OR, USA) sampling at 120 Hz tracked the position of four reflective markers attached rigidly to the surface of the IMU. Both the IMU and OMC systems were calibrated using manufacturer-specified procedures, including removing initial gyroscope bias using the manufacturer's software. The OMC measurements were recorded for the duration of each trial (1 min). The IMU measurements were recorded for the entirety of each testing session (>30 min).

#### 2.2.3. Optical motion capture

The OMC provides a quaternion $\vec{q}_b^{\,n}$ describing the spatial orientation of a given rigid body $b$ relative to frame $n$. $\vec{g}_k$ is obtained from OMC using (*19*) in Appendix C. Note that $\vec{g}_k$ corresponds to the direction of gravity in the body frame (i.e., perfect accelerometer measurement), assuming that frame $n$ is aligned with the gravity vector. Once $\vec{g}_k$ was obtained, incVel was calculated using (*1*) and (*2*), and VDGV was calculated using (*3*). These measurements will be referred to as omc-incVel and omc-VDGV. Further, $\vec{\omega}_k$ was calculated from OMC using (*20*) and will be referred to as omc-GVM. The three OMC-based measurements were used as reference signals with which to compare the sensor-based measurements.

#### 2.2.4. Inertial measurement unit

The raw accelerometer data were first low-pass filtered (2nd order Butterworth, 5 Hz corner frequency). Then, $\vec{g}_k$ was calculated by normalizing the filtered accelerometer measurements before using (*1*) and (*2*) to calculate incVel (acc-incVel), and (*3*) to calculate VDGV (acc-VDGV).

IMU-derived measurements were obtained using a Kalman Filter with gyroscope bias estimation to combine raw accelerometer and gyroscope data. Details of the algorithm and its tuning coefficients can be found elsewhere (Chen et al., 2020). The Kalman Filter output provides the direction of gravity in the sensor frame theoretically unaffected by increased motion speeds. Similar to omc-incVel and omc-VDGV, $\vec{g}_k$ is obtained from IMU using (*19*) in Appendix C before using (*1*) and (*2*) to calculate incVel (imu-incVel) and (*3*) to calculate VDGV (imu-VDGV). The GVM was calculated directly from unfiltered angular velocity data from the IMU's gyroscope. This measurement will be referred to as imu-GVM.

#### 2.2.5. Angular velocity accuracy assessment

Consistent with our previous studies (Chen et al., 2018, 2020), the offset between the local OMC coordinate frame and the local IMU coordinate frame was determined using angular velocity measurements according to de Vries et al. (2009). The calculated local offset was applied to the OMC measurements, and the offset between the OMC reference frame (lab coordinate frame) and the reference IMU coordinate frame (gravity and initial heading) was subsequently calculated under static conditions using Accel-derived inclination measurements and then applied to OMC measurements. The offsets were applied to OMC measurements to control for differences in offsets affecting results from IMU- and Accel-derived velocities.

Peak error was defined as the 99th percentile measurement of the rectified sample-to-sample difference between the reference (OMC) and sensor-derived measurements. RMS error was calculated as follows:

$$\mathrm{RMS} = \sqrt{\frac{1}{n}\sum\left(\dot{\alpha}_{omc} - \dot{\alpha}_{sensor}\right)^2} \tag{7}$$

where $\dot{\alpha}_{sensor}$ is the sensor-derived angular velocity (i.e., acc-incVel, imu-incVel, acc-VDGV, imu-VDGV, or imu-GVM) and $\dot{\alpha}_{omc}$ is the corresponding angular velocity calculated from the OMC (i.e., omc-incVel, omc-VDGV, or omc-GVM). Note that the calculation of VDGV measurements rectifies angular velocity.

## 3. Results

As expected, greater angular velocities were observed using omc-GVM compared to omc-VDGV and omc-incVel. Across participants and transfer rates, the mean omc-VDGV was 89% of the mean omc-GVM, and the mean omc-incVel was 77% of the mean omc-GVM. The same trend (i.e., GVM > VDGV > incVel) was observed for the IMU- and accelerometer-based approaches averaged across all transfer rates for the 10th, 50th, 90th, and 99th percentiles of the measured angular velocity values (Fig. 1). The angular velocities calculated using omc-GVM, omc-VDGV, omc-incVel, imu-GVM, imu-VDGV, and acc-VDGV from 5 s of a single trial with a 'fast' transfer rate are shown in Fig. 2.

Mean RMS and peak angular velocity errors by transfer rate, angular velocity calculation method, sensing modality, and reference signal are shown in Table 1. Using omc-GVM as the reference, RMS and peak errors for omc-VDGV were about 18°/s and 56°/s, respectively, for the 'fast' transfer rate. RMS and peak errors for omc-incVel were about 32°/s and 89°/s, respectively. These results provide empirical support for the notion that, in the absence of error introduced through the use of accelerometer data, VDGV yields lower measurement error than incVel.

Theoretically, then, and assuming omc-VDGV is the "true" VDGV (i.e., as the reference signal), one would expect to observe lower error for acc-VDGV than for acc-incVel. However, acc-VDGV and acc-incVel exhibited similar RMS and peak errors at the 'slow' transfer rate and, at both the 'medium' and 'fast' transfer rates, both RMS and peak errors were lower for acc-incVel than for acc-VDGV (e.g., at the 'fast' transfer rate, peak error was about 154°/s for acc-incVel but about 230°/s for acc-VDGV). As expected, incorporating the gyroscope and sensor fusion dramatically reduced error relative to the omc-VDGV reference. For example, at the 'fast' transfer rate, the peak error for imu-VDGV was about 33°/s compared to 230°/s for acc-VDGV.

Relative to omc-GVM, imu-GVM yielded the lowest error among all sensor-based approaches for angular velocity measurement considered in this study. Error magnitudes for imu-GVM were also the least susceptible to influence from motion speed. The mean RMS error of imu-GVM increased from 3.5°/s at the 'slow' transfer rate to 8.3°/s at the 'fast' transfer rate (a 2.4-fold increase). In contrast, the mean RMS error of imu-VDGV increased from 7.7°/s to 20.1°/s (a 2.6-fold increase), the mean RMS error of imu-incVel increased from 12.4°/s to 34.2°/s (a 2.8-fold increase), the mean RMS error of acc-incVel increased from 15.3°/s to 69.5°/s (a 4.5-fold increase), and the mean RMS error of acc-VDGV increased from 12.6°/s to 76.5°/s (a 6.1-fold increase). The mean peak error was also the lowest for imu-GVM across all transfer rates, with an increase from 11.4°/s at the 'slow' transfer rate to 27.9°/s at the 'fast' transfer rate (a 2.6-fold increase). The mean peak errors for imu-VDGV and imu-incVel were greater than for imu-GVM. However, the proportional increases observed were similar (i.e., 2.3-fold for imu-VDGV and 2.2-fold for imu-incVel). In addition to greater mean peak error than imu-GVM, the proportional increases for acc-VDGV and acc-incVel were more dramatic (i.e., 4.9-fold for acc-VDGV and 3.4-fold for acc-incVel).

## 4. Discussion

Both acc-incVel and acc-VDGV were conceived as methods to measure the speed of body segments in occupational health studies when miniature, inexpensive gyroscopes were not prevalent in wearable devices. However, acc-incVel and acc-VDGV have two inherent limitations: (i) the angular velocities captured do not reflect the full extent of motion (confirmed in this study with mean omc-incVel and omc-VDGV velocities that are 77% and 89% of the mean omc-GVM velocities), and (ii) the accuracy of accelerometer-based angular velocity measurements is reduced as motion speeds increase (indicated in this study as a ~103°/s increase in peak error of acc-incVel [vs. omc-incVel] and a ~195°/s increase in peak error of acc-VDGV [vs. omc-VDGV] from the slow to fast transfer rates). Using GVM addresses both limitations, as indicated by (i) peak errors of <30°/s in imu-GVM [vs. omc-GVM] across all motion speeds, and (ii) just a ~16°/s increase in peak error from the slow to fast transfer rates.

Although all three accelerometer axes are used in the calculations of both incVel and VDGV, neither method captures all three directions of motion. For example, pure rotation around gravity will yield zero angular velocity when calculated using either VDGV or incVel. VDGV may be preferable to incVel since it captures a fuller extent of motion. However, the results of the current study suggest some important methodological limitations. We did not expect greater error for acc-VDGV compared to acc-incVel when considering omc-VDGV as the reference (for the 'medium' and 'fast' transfer rates). We believe the most likely explanation for this result is a 'compounding' of accelerometer error across multiple movement directions (i.e., two movement directions with VDGV vs. one with incVel) as motion speeds increase. Although the inclusion of a gyroscope and sensor fusion (i.e., imu-VDGV and imu-incVel) resulted in superior error characteristics, these approaches can still not capture rotation around gravity.

The results of this study verify that angular velocity measurements calculated using GVM encompass all movement directions and can be easily calculated using measurements from field-capable IMUs. When omc-GVM was used as the reference, imu-GVM produced the most accurate sensor-based angular velocity measurements, with peak errors <27.9°/s across all transfer rates. This is in contrast to acc-VDGV measurements, which theoretically better represents the "true" angular velocity compared to incVel but may not empirically as indicated in this study. Errors associated with angular velocities measured from gyroscopes are time-invariant and that gyroscopic drift is introduced when gyroscope measurements are integrated with respect to time to obtain spatial orientation without the use of a sensor fusion algorithm. Although omc-GVM was used as the reference, we hypothesize that the slight increase in imu-GVM errors with increased transfer rates may be attributed to the differentiation of OMC-derived orientation measurements with respect to time, which itself introduces error that may be magnified as the transfer rate increased. It is conceivable that the OMC can produce more accurate orientation measurements while the gyroscope produces more accurate angular velocities.

The relative magnitude between GVM, VDGV, and incVel measurements is generally difficult to compare across studies due to differences in motion patterns. GVM, VDGV, and incVel will produce identical

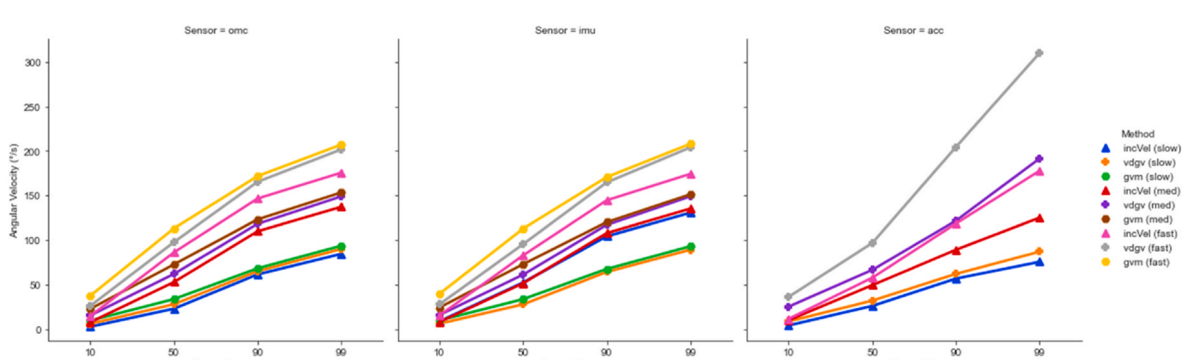


**Fig. 1.** Mean 10th, 50th, 90th, and 99th percentile angular velocities for each sensing modality (optical motion capture [omc], inertial measurement unit [imu], and accelerometer [acc]) and angular velocity calculation method (gyroscope vector magnitude [gvm], vector-differenced generalized velocity [vdgv], and inclination velocity [incVel]) for 'slow', 'medium', and 'fast' transfer rates.

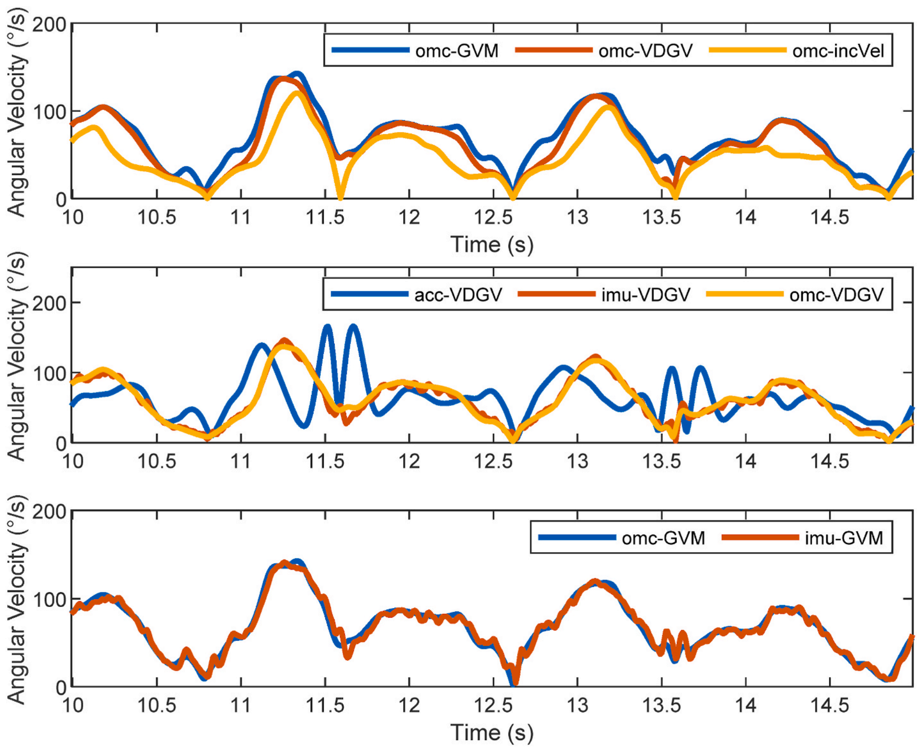


**Fig. 2.** [top]: Optical motion capture-derived angular velocities from 5 s of a single trial with 'fast' transfer rate calculated using gyroscope vector magnitude (omc-GVM), vector-differenced generalized velocity (omc-VDGV), and inclination velocity (omc-incVel). [middle]: omc-VDGV, vector-differenced generalized velocities measured from an inertial measurement unit (imu-VDGV), and accelerometer (acc-VDGV) from the corresponding trial. [bottom]: omc-GVM and gyroscope vector magnitude calculated from a gyroscope contained within the inertial measurement unit (imu-GVM).

**Table 1**

Mean(SD) root-mean-square and peak error angular velocities across 13 participants and various transfer rates calculated using three different methods: gyroscope vector magnitude calculated using optical motion capture (omc-GVM), inertial measurement unit (imu-GVM); vector-differenced generalized velocity (VDGV) using optical motion capture (omc-VDGV), inertial measurement unit (imu-VDGV), accelerometer (acc-VDGV); inclination velocity calculated using optical motion capture (omc-incVel), inertial measurement unit (imu-incVel), and accelerometer (acc-incVel).

| | Reference Computational Method | | | | | |
|---|---|---|---|---|---|---|
| | omc-GVM | | omc-VDGV | | omc-incVel | |
| | RMS error (°/s) | Peak error (°/s) | RMS error (°/s) | Peak error (°/s) | RMS error (°/s) | Peak error (°/s) |
| | Mean (sd) | Mean (sd) | Mean (sd) | mean (sd) | mean (sd) | mean (sd) |
| **'Slow' Rate** | | | | | | |
| omc-VDGV | 7.0(1.8) | 25.0(6.5) | -REF- | -REF- | 7.3(2.9) | 29.2(12.5) |
| omc-incVel | 12.0(3.2) | 40.8(12.8) | 7.3(2.9) | 29.2(12.5) | -REF- | -REF- |
| imu-GVM | 3.5(0.7) | 11.4(2.6) | 7.8(1.9) | 26.2(6.9) | 12.7(3.2) | 43.6(13.3) |
| imu-VDGV | 7.7(1.8) | 25.5(6.3) | 3.5(1.1) | 11.9(4.1) | 8.2(2.8) | 31.8(12.3) |
| acc-VDGV | 12.6(2.6) | 41.8(11.7) | 13.0(3.1) | 44.9(13.8) | 15.7(3.8) | 56.3(18.2) |
| imu-incVel | 12.4(3.2) | 40.5(12.5) | 8.0(2.7) | 29.9(12.0) | 3.0(1.0) | 9.6(3.8) |
| acc-incVel | 15.3(3.1) | 47.5(12.6) | 13.0(3.0) | 41.7(11.9) | 11.7(2.6) | 38.4(10.0) |
| **'Medium' Rate** | | | | | | |
| omc-VDGV | 12.9(3.1) | 42.4(10.4) | -REF- | -REF- | 14.3(5.1) | 53.0(21.8) |
| omc-incVel | 22.6(6.1) | 67.7(21.1) | 14.3(5.1) | 53.0(21.8) | -REF- | -REF- |
| imu-GVM | 5.7(1.4) | 18.8(5.8) | 14.4(3.2) | 46.5(11) | 24.1(6.5) | 77.0(24.7) |
| imu-VDGV | 14.0(2.8) | 43.7(9.8) | 6.5(1.6) | 22.2(6.5) | 15.7(5.0) | 58.5(21.4) |
| acc-VDGV | 39.2(11.5) | 117.3(40.3) | 43.3(12.8) | 134.0(46.5) | 48.3(15.2) | 152.4(53.9) |
| imu-incVel | 23.6(5.7) | 68.1(19.9) | 15.4(4.6) | 52.7(19.1) | 5.4(1.4) | 16.0(4.5) |
| acc-incVel | 39.1(9.3) | 104.6(20.5) | 35.6(9.7) | 97.9(21.8) | 32.7(9.8) | 92.9(24.3) |
| **'Fast' Rate** | | | | | | |
| omc-VDGV | 17.7(8.1) | 55.6(23.4) | -REF- | -REF- | 21.2(7.6) | 71.0(25.4) |
| omc-incVel | 32.3(11.4) | 89.4(30.7) | 21.2(7.6) | 71.0 (25.4) | -REF- | -REF- |
| imu-GVM | 8.3(1.7) | 27.9(6.9) | 20.7(7.4) | 64.8(21.1) | 34.9(11.3) | 103.7(32.3) |
| imu-VDGV | 20.1(7.2) | 59.5(22) | 9.9(2.3) | 32.9(9.4) | 23.7(7.2) | 81.4(25.0) |
| acc-VDGV | 76.5(20.4) | 205.3(66.4) | 83.0(23.6) | 230.6(77.5) | 87.4(27.2) | 251.3(88.3) |
| imu-incVel | 34.2(10.6) | 90.9(28) | 23.3(6.9) | 72.0 (22.2) | 8.0 (2) | 23.1(6.9) |
| acc-incVel | 69.5 (15.2) | 159.9(30.5) | 64.2(13.0) | 154.4(29.0) | 57.4(11.9) | 141.0(25.1) |

results with planar motion in the direction of incVel. However, only GVM will register angular velocities when motion occurs purely around gravity. To our knowledge, Fan et al. (2021) provided the only comparable study and reported that the mean upper arm imu-VDGV was 16.5°/s greater than the mean upper arm imu-IncVel during manual material handling activities. In our study, the mean omc-VDGV was 4.2°/s, 8.7°/s, and 13.8°/s greater than the mean omc-incVel for the 'slow,' 'medium,' and 'fast' transfer rates, respectively. We hypothesize that these differences may be attributed to differences in motion patterns. In our study, a short-duration, cyclic task was performed in contrast to actual material handling tasks, which are likely to involve greater motion complexity. Furthermore, Fan et al. (2021) calculated VDGV and IncVel using sensor fusion from IMU measurements. Although sensor fusion substantially reduces the effects of increased motion speeds (i.e, increased non-gravitational acceleration) on angular velocity accuracy, the presence of non-gravitational acceleration will adversely affect the accuracy of angular velocities derived from vector measurements since accelerometer measurements are used. Fan et al. (2021) reported acc-VDGV mean and percentile measurements generally greater than imu-VDGV, with the 90th and 99th percentile acc-VDGV exceeding imu-VDGV by over 100°/s and 200°/s, respectively. The results were consistent with our study, which indicated that acc-VDGV mean and percentile measurements were generally greater than imu-VDGV, with observed percentile differences >100°/s. However, in our study, the difference between mean imu-VDGV and acc-VDGV was <15°/s across all transfer rates, in contrast to the 50°/s difference observed in Fan et al. (2021) despite a mean imu-VDGV that was lower than our 'medium' transfer rate. We again hypothesize that our observed differences between VDGV and incVel are smaller since our motion pattern was less complex.

### *4.1. Strengths and limitations*

An important strength of the current study is our use of OMC measurements for comparing GVM, VDGV, and incVel, which provided 'true' reference signals for comparison (Cuesta-Vargas et al., 2010) and controlled for potential IMU errors when evaluating angular velocity calculation methods. The comparisons of acc-VDGV and imu-VDGV to omc-VDGV also highlight potential inaccuracies of acc-VDGV and the improvements that can be achieved through sensor fusion (Chen et al., 2018, 2020). Furthermore, the derivations provided a geometric explanation for a quantity of angular velocity sometimes found in the literature (i.e., GVM) and how it relates to the generalized velocity calculations often used to estimate movement velocities in studies of occupational health. A limitation of this paper is the relatively simplistic motion pattern. We expect differences between GVM, VDGV, and incVel to be accentuated as motion complexity increases. Furthermore, the error magnitudes observed may not generalize to a field-based study (i. e., in a workplace) since the motion speeds tested are unlikely to be sustained beyond a few minutes.

Ultimately, all single-sensor solutions for measuring upper arm angular velocity have limitations without information about the relative motion between the upper arm and torso. For example, GVM may overestimate the 'true' angular velocity for work activities that include a substantial amount of torso rotation (i.e., twisting). At the same time, VDGV may underestimate the 'true' angular velocity since no motion in the horizontal plane is considered. While a two-sensor solution (e.g., torso IMU and upper arm IMU) may improve the accuracy of upper arm velocity measurement, a single-sensor solution may maximize worker (and/or employer) acceptance, minimize setup time, or afford collection of exposure information among a greater sample of workers given limited time and resources.

### *4.2. Methodological considerations for future studies*

When considering historical data captured with accelerometers, the difference between acc-incVel and acc-VDGV may not be appreciable, particularly at high movement speeds. In these cases, acc-incVel will likely produce angular velocities more representative of 'true' VDGV than acc-VDGV, given the sensitivity of acc-VDGV to non-gravitational acceleration. Furthermore, the implication that acc-VDGV tends to over-estimate velocities compared to omc-VDGV, particularly near the extremes of the angular velocity distribution (e.g., the 90th and 99th percentiles), could contribute to error in the estimates of the dose-response relationship between exposures to high angular velocities and WMSDs, such as those provided by Arvidsson et al. (2021). The differences in imu-VDGV and acc-VDGV may also result in difficulties when comparing angular velocities across historical studies. Angular velocities calculated using imu-VDGV may, for example, be considered 'safe' according to proposed threshold limit values while considered 'exposed' when derived from acc-VDGV.

We suggest GVM as a new angular velocity calculation method in future studies since it captures all three motion directions, is theoretically unaffected by either increased motion speeds or measurement duration and is simpler to calculate than VDGV since it does not require sensor fusion to provide accurate angular velocities. An important question is whether the use of GVM as a measure of upper arm angular velocity in epidemiological studies reduces the potential for systematic error in exposure estimation or improves the precision of risk estimates in comparison to either incVel or VDGV approaches. These questions motivate, at least partially, the recent work by Forsman et al. (2022a, 2022b) and Fan et al. (2021) to develop models for converting exposure estimates based on incVel to exposure estimates based on VDGV (and vice versa).

We also suggest quantifying imu-VDGV, accel-VDGV, imu-incVel, and acc-incVel in addition to GVM to facilitate these comparisons. The additional information provided in Appendix D can aid this process, particularly refining conversion models that have been previously proposed (Forsman et al., 2022b). Future research should evaluate both single-sensor and two-sensor solutions for quantifying angular velocities of the upper arm and examine the associations of each with shoulder MSDs.

## Declaration of competing interest

The authors declare that they have no known competing financial interests or personal relationships that could have appeared to influence the work reported in this paper.

## Acknowledgments

This study was supported by research funding from the Centers for Disease Control (CDC)/National Institute for Occupational Safety and Health (NIOSH). This included funding from the Heartland Center for Occupational Health and Safety at the University of Iowa (T42OH008491), the Deep South Center for Occupational Health and Safety at the University of Alabama-Birmingham (UAB) and Auburn University (T42OH008436). The findings and conclusions in this report are those of the authors and do not necessarily represent the views of the CDC/NIOSH.

## Appendix A. Quaternion Basics

Rotating a 3-dimensional vector from frame b ($\vec{x}^{b}$) to frame a ($\vec{x}^{a}$) is accomplished as follows:

$$\begin{bmatrix} 0 \\ \vec{x}^{a} \end{bmatrix} = \vec{q}^{\,a}_{b} \otimes \begin{bmatrix} 0 \\ \vec{x}^{b} \end{bmatrix} \otimes \vec{q}^{\,a'}_{b} \tag{8}$$

$$\vec{a} \otimes \vec{b} = \begin{bmatrix} a_0 \\ \vec{\boldsymbol{a}} \end{bmatrix} \otimes \begin{bmatrix} b_0 \\ \vec{\boldsymbol{b}} \end{bmatrix} = \begin{bmatrix} a_0 & -\vec{\boldsymbol{a}}^T \\ \vec{\boldsymbol{a}} & a_0 I_3 + [\vec{\boldsymbol{a}}]_\times \end{bmatrix} \tag{9}$$

$$\vec{q}^{\,\prime} = \begin{bmatrix} q_0 \\ -\vec{\boldsymbol{q}} \end{bmatrix} \tag{10}$$

where $\otimes$ is the quaternion product, $\vec{q}^{\,\prime}$ is the quaternion conjugate of $\vec{q}$, $[\bullet]_\times$ is the skew symmetric operator, and $I_3$ is a $3 \times 3$ identity matrix.

Similarly, rotating a 3-dimensional vector from frame a to frame b is achieved as follows:

$$\begin{bmatrix} 0 \\ \vec{x}^b \end{bmatrix} = \vec{q}_b^{\,a\prime} \otimes \begin{bmatrix} 0 \\ \vec{x}^a \end{bmatrix} \otimes \vec{q}_b^{\,a} \tag{11}$$

Given $\vec{q}_b^{\,a}$, which describes the rotation from frame b to frame a, and $\vec{q}_c^{\,b}$, which describes the rotation from frame c to frame b, $\vec{q}_c^{\,a}$, which describes the rotation from frame c to frame a, is calculated as follows:

$$\vec{q}_c^{\,a} = \vec{q}_b^{\,a} \otimes \vec{q}_c^{\,b} \tag{12}$$

Similarly, given $\vec{q}_b^{\,a}$ and $\vec{q}_c^{\,a}$, $\vec{q}_c^{\,b}$ can be obtained as follows:

$$\vec{q}_c^{\,b} = \vec{q}_b^{\,a\prime} \otimes \vec{q}_c^{\,a} \tag{13}$$

## Appendix B. Defining Gyroscope Vector Magnitude

From Equations (*12*) and (*13*), $\vec{q}_{b,k-1}^{\,n}$ and $\vec{q}_{b,k}^{\,n}$ can be defined as the orientation at instance k-1 and k relative to a common reference frame $n$, and $q_{b,k}^{b,k-1}$ can be defined as the orientation of $\vec{q}_{b,k}^{\,n}$ relative to $\vec{q}_{b,k-1}^{\,n}$. Given an initial orientation and perfect angular velocities in the sensor frame, angular velocities can be integrated with respect to time by applying Equation (*14*) recursively to calculate subsequent orientation (Brodie et al., 2008).

$$\vec{q}_{b,k}^{\,n} = \vec{q}_{b,k-1}^{\,n} \otimes \vec{q}_{b,k}^{\,b,k-1} \tag{14}$$

Since $\vec{q}_{b,k}^{\,b,k-1}$ describes the orientation, it can be decomposed into a direction specified by the unit vector $\vec{u}$ and angle $\eta$ (*15*). When $\vec{q}_{b,k}^{\,b,k-1}$ is determined using angular velocity measurements in the sensor frame (i.e., gyroscope measurements), $\vec{u}$ is calculated by normalizing $\vec{\varpi}$ to unitary (*16*) and $\eta$ is determined by multiplying the vector magnitude of $\vec{\varpi}$ by its sample period ($\Delta t$), as seen in Equation (*18*). $\eta$ can be therefore be defined as the net directional change between successive measurements of orientation.

$$q_{b,k}^{b,k-1} = \begin{bmatrix} \cos(\eta/2) \\ \vec{u}\sin(\eta/2) \end{bmatrix} \tag{15}$$

$$\vec{u} = \frac{\vec{\varpi}}{\|\vec{\varpi}\|_2} \tag{16}$$

$$\eta = \|\vec{\varpi}\|_2 \Delta t \tag{17}$$

$$\dot{\eta} = \frac{\eta}{\Delta t} = \|\vec{\varpi}\|_2 \tag{18}$$

Dividing $\eta$ by its sample period would yield the rate of directional change between successive measurements of orientation ($\dot{\eta}$), also known as the angular velocity. Therefore, the vector magnitude of gyroscope measurements can be defined as the rate of directional change between successive orientation measurements.

## Appendix C. Calculating gravitational vector and angular velocities from a quaternion

An OMC or the sensor fusion output from an IMU will provide quaternion $\vec{q}_b^{\,n}$, which describes the spatial orientation of a given rigid body ($b$) relative a reference frame ($n$). Given $\vec{q}_b^{\,n}$, $\vec{g}_k$ can be calculated by applying (*11*) as follows:

$$\begin{bmatrix} 0 \\ \vec{g}_k \end{bmatrix} = \vec{q}_{b,k}^{\,n\;\prime} \otimes \begin{bmatrix} 0 \\ 0 \\ 0 \\ 1 \end{bmatrix} \otimes \vec{q}_{b,k}^{\,n} \tag{19}$$

Given $\vec{q}_{b,k-1}^{\,n}$ and $\vec{q}_{b,k}^{\,n}$, and $\Delta t$, $\vec{\varpi}_k$ can be calculated as follows:

$$\vec{\varpi}_k = \vec{u}\|\vec{\varpi}\|_2 \tag{20}$$

$$\vec{u} = \frac{\Delta\vec{\boldsymbol{q}}}{\sin(\eta/2)} \tag{21}$$

$$\eta = 2\ \mathrm{acos}(\Delta q_0) \tag{22}$$

$$\|\vec{\omega}\|_2 = \frac{\eta}{\Delta t} \tag{23}$$

$$\Delta\vec{q} = \begin{bmatrix} \Delta q_0 \\ \Delta q_1 \\ \Delta q_2 \\ \Delta q_3 \end{bmatrix} = \begin{bmatrix} \Delta q_0 \\ \Delta \vec{\boldsymbol{q}} \end{bmatrix} = \vec{q}^{\,n'}_{b,k-1} \otimes \vec{q}^{\,n}_{b,k} \tag{24}$$

## Appendix D. Angular velocity summary metrics

**Table 2**
Mean(SD) angular velocities across 13 participants and various transfer rates calculated using various methods: gyroscope vector magnitude calculated using optical motion capture (omc-GVM), inertial measurement unit (imu-GVM); vector-differenced generalized velocity (VDGV) using optical motion capture (omc-VDGV), inertial measurement unit (imu-VDGV), accelerometer (acc-VDGV); inclination velocity calculated using optical motion capture (omc-incVel), inertial measurement unit (imu-incVel), and accelerometer (acc-incVel).

| | omc-GVM | imu-GVM | omc-VDGV | imu-VDGV | acc-VDGV | omc-incVel | imu-incVel | acc-incVel |
|---|---|---|---|---|---|---|---|---|
| **'Slow' Transfer Rate** | | | | | | | | |
| Mean (°/s) | 36.6(2.9) | 36.5(2.9) | 32.2(2.7) | 32.0(2.6) | 34.0(3.1) | 28.2(2.1) | 27.7(2.0) | 28.6(2.3) |
| 5th Percentile (°/s) | 6.5(2.5) | 6.8(2.7) | 3.7(1.6) | 3.9(1.7) | 5.8(1.7) | 1.3(0.6) | 1.3(0.6) | 2.1(0.7) |
| 10th Percentile (°/s) | 9.5(3.5) | 9.7(3.5) | 5.8(2.3) | 6.0(2.4) | 8.5(2.2) | 2.6(1.1) | 2.7(1.2) | 4.0(1.3) |
| 25th Percentile (°/s) | 17.2(4.7) | 17.5(4.7) | 12.0(3.7) | 12.4(3.6) | 16.3(2.8) | 7.4(2.7) | 7.6(2.6) | 10.6(2.5) |
| 50th Percentile (°/s) | 33.5(4.0) | 33.5(4.0) | 27.8(3.8) | 27.7(3.5) | 31.9(3.4) | 22.8(3.8) | 22.5(3.4) | 25.9(2.7) |
| 75th Percentile (°/s) | 53.3(5.2) | 52.8(5.1) | 49.7(4.8) | 48.9(4.7) | 49.0(5.1) | 46.2(5.0) | 45.2(4.7) | 44.4(4.6) |
| 90th Percentile (°/s) | 68.1(9.0) | 67.4(8.8) | 64.9(8.8) | 64.1(8.7) | 61.9(7.5) | 61.3(8.7) | 60.1(8.4) | 56.6(7.0) |
| 99th Percentile (°/s) | 93.4(16.4) | 92.9(16.5) | 89.9(15.9) | 89.1(16.0) | 86.9(14.7) | 84.4(14.5) | 82.4(14.1) | 75.5(10.7) |
| Time at low velocities (<5°/s)(%) | 4.0(2.7) | 3.7(2.6) | 9.5(4.4) | 9.1(4.3) | 4.6(2.5) | 19.5(6.4) | 19.0(6.2) | 13.2(3.7) |
| Time at high velocities (≥90°/s)(%) | 2.1(2.5) | 2.0(2.4) | 1.6(2.0) | 1.5(1.9) | 1.1(1.4) | 1.0(1.5) | 0.9(1.4) | 0.4(0.6) |
| **'Medium' Transfer Rate** | | | | | | | | |
| Mean (°/s) | 72.7(6.7) | 72.5(6.8) | 64.6(5.8) | 64.1(5.9) | 70.7(8.1) | 56.0(5.3) | 55.0(5.3) | 49.7(5.9) |
| 5th Percentile (°/s) | 15.8(5.3) | 16.3(5.4) | 9.8(3.8) | 10.4(4.1) | 17.2(5.7) | 3.6(1.5) | 3.8(1.5) | 4.9(1.7) |
| 10th Percentile (°/s) | 22.6(6.5) | 23.2(6.6) | 15.1(5.3) | 15.6(5.7) | 25.1(6.7) | 7.5(2.8) | 7.8(2.8) | 9.8(3.0) |
| 25th Percentile (°/s) | 40.5(8.8) | 41.0(8.8) | 30.1(7.3) | 30.6(7.5) | 43.2(6.5) | 20.4(6.0) | 20.7(5.9) | 24.7(5.8) |
| 50th Percentile (°/s) | 72.5(7.3) | 72.2(7.4) | 61.8(6.4) | 61.1(6.3) | 66.4(7.2) | 52.6(6.2) | 51.4(5.9) | 49.3(7.2) |
| 75th Percentile (°/s) | 102.3(13.1) | 101.3(13.1) | 95.8(12.0) | 94.0(12.0) | 90.1(12.1) | 88.3(12.9) | 85.8(12.3) | 70.7(8.2) |
| 90th Percentile (°/s) | 123.1(15.2) | 122.0(15.3) | 118.1(15.0) | 116.9(14.8) | 121.6(24.6) | 109.7(17.3) | 107.7(16.8) | 89.0(11.2) |
| 99th Percentile (°/s) | 153.3(17.3) | 152.8(17.0) | 148.8(17.9) | 149.0(17.7) | 191.6(53.4) | 137.1(19.1) | 135.2(18.7) | 125.1(20.4) |
| Time at low velocities (<5°/s)(%) | 0.6(0.7) | 0.6(0.7) | 2.4(2.1) | 2.2(2.1) | 0.8(0.8) | 7.9(3.8) | 7.6(3.7) | 5.7(2.0) |
| Time at high velocities (≥90°/s)(%) | 34.1(7.4) | 33.4(7.8) | 28.1(7.0) | 26.9(7.4) | 24.4(9.2) | 21.7(8.5) | 20.2(8.7) | 9.8(6.0) |
| **'Fast' Transfer Rate** | | | | | | | | |
| Mean (°/s) | 108.5(14.2) | 108.8(14.5) | 97.0(10.5) | 96.4(11.0) | 109.2(18.6) | 83.3(9.8) | 81.5(9.8) | 62.5(7.2) |
| 5th Percentile (°/s) | 26.2(10.3) | 28.3(10.2) | 16.8(4.5) | 18.0(5.7) | 24.5(3.7) | 7.3(1.8) | 7.5(2.6) | 5.8(1.4) |
| 10th Percentile (°/s) | 37.3(12.2) | 39.4(12.3) | 25.9(5.9) | 27.6(7.2) | 36.1(4.2) | 14.5(3.1) | 15.1(4.0) | 11.4(2.5) |
| 25th Percentile (°/s) | 66.9(14.2) | 68.2(14.3) | 52.5(8.3) | 53.1(8.9) | 60.6(5.6) | 39.1(4.9) | 39.6(5.3) | 28.7(5.3) |
| 50th Percentile (°/s) | 112.9(15.4) | 112.7(15.3) | 97.5(12.1) | 95.3(12.2) | 96.6(14.5) | 86.0(10.6) | 82.7(10.4) | 57.6(7.6) |
| 75th Percentile (°/s) | 148.4(18.8) | 147.4(19.4) | 139.3(16.4) | 137.3(17.1) | 141.9(28.2) | 125.1(17.5) | 121.5(17.3) | 89.5(10.3) |
| 90th Percentile (°/s) | 171.7(21.4) | 170.6(22.1) | 165.3(19.7) | 164.7(20.9) | 204.4(49.6) | 146.5(20.1) | 144.6(20.2) | 118.5(16.6) |
| 99th Percentile (°/s) | 207.1(23.8) | 208.0(25.0) | 201.7(23.8) | 204.0(25.0) | 310.1(77.6) | 175.5(20.9) | 174.2(21.4) | 177.8(30.5) |
| Time at low velocities (<5°/s)(%) | 0.1(0.1) | 0.1(0.1) | 0.7(0.4) | 0.7(0.4) | 0.2(0.2) | 3.6(0.9) | 3.6(0.9) | 4.6(1.3) |
| Time at high velocities (≥90°/s)(%) | 62.5(7.8) | 62.9(8.1) | 54.0(6.0) | 52.9(6.5) | 52.3(8.0) | 46.7(6.1) | 44.6(6.5) | 24.1(6.9) |

## References


Arvidsson, I., Balogh, I., Hansson, G.-Å., Ohlsson, K., Åkesson, I., Nordander, C., 2012. Rationalization in meat cutting – Consequences on physical workload. Appl. Ergon. 43, 1026–1032. https://doi.org/10.1016/j.apergo.2012.03.001.

Arvidsson, I., Dahlqvist, C., Enquist, H., Nordander, C., 2021. Action levels for the prevention of work-related musculoskeletal disorders in the neck and upper extremities: a proposal. Ann. Work Exposures Health 65, 741–747. https://doi.org/10.1093/annweh/wxab012.

Balogh, I., Arvidsson, I., Björk, J., Hansson, G.-Å., Ohlsson, K., Skerfving, S., Nordander, C., 2019. Work-related neck and upper limb disorders – quantitative exposure–response relationships adjusted for personal characteristics and psychosocial conditions. BMC Muscoskel. Disord. 20, 139. https://doi.org/10.1186/s12891-019-2491-6.

Bernmark, E., Wiktorin, C., 2002. A triaxial accelerometer for measuring arm movements. Appl. Ergon. 33, 541–547. https://doi.org/10.1016/S0003-6870(02)00072-8.

Brodie, M.a., Walmsley, A., Page, W., 2008. Dynamic accuracy of inertial measurement units during simple pendulum motion. Comput. Methods Biomech. Biomed. Eng. 11, 235–242. https://doi.org/10.1080/10255840802125526.

Chen, H., Schall, M.C., Fethke, N., 2018. Accuracy of angular displacements and velocities from inertial-based inclinometers. Appl. Ergon. 67, 151–161. https://doi.org/10.1016/j.apergo.2017.09.007.

Chen, H., Schall, M.C., Fethke, N., 2017. Effects of movement speed and magnetic disturbance on the accuracy of inertial measurement units. Proc. Hum. Factors Ergon. Soc. Annu. Meet. 61, 1046–1050. https://doi.org/10.1177/1541931213601745.

Chen, H., Schall, M.C., Fethke, N.B., 2020. Measuring upper arm elevation using an inertial measurement unit: an exploration of sensor fusion algorithms and gyroscope models. Appl. Ergon. 89, 103187 https://doi.org/10.1016/j.apergo.2020.103187.

Cuesta-Vargas, A.I., Galán-Mercant, A., Williams, J.M., 2010. The use of inertial sensors system for human motion analysis. Phys. Ther. Rev. 15, 462–473. https://doi.org/10.1179/1743288X11Y.0000000006.

de Vries, W.H.K., Veeger, H.E.J., Baten, C.T.M., van der Helm, F.C.T., 2009. Magnetic distortion in motion labs, implications for validating inertial magnetic sensors. Gait Posture 29, 535–541. https://doi.org/10.1016/j.gaitpost.2008.12.004.

Douphrate, D.I., Fethke, N.B., Nonnenmann, M.W., Rosecrance, J.C., Reynolds, S.J., 2012. Full shift arm inclinometry among dairy parlor workers: a feasibility study in a challenging work environment. Appl. Ergon. 43, 604–613. https://doi.org/10.1016/j.apergo.2011.09.007.

Fan, X., Lind, C.M., Rhen, I.-M., Forsman, M., 2021. Effects of sensor types and angular velocity computational methods in field measurements of occupational upper arm and trunk postures and movements. Sensors 21, 5527. https://doi.org/10.3390/s21165527.

Forsman, M., Fan, X., Rhén, I.-M., Lind, C.M., 2022a. Concerning a Work Movement Velocity Action Level Proposed in "Action Levels for the Prevention of Work-Related Musculoskeletal Disorders in the Neck and Upper Extremities: a Proposal" by Inger Arvidsson et al. (2021). Ann. Work Exposures Health 66, 130–131. https://doi.org/10.1093/annweh/wxab075.

Forsman, M., Fan, X., Rhen, I.-M., Lind, C.M., 2022b. Mind the gap – development of conversion models between accelerometer- and IMU-based measurements of arm and trunk postures and movements in warehouse work. Appl. Ergon. 105, 103841 https://doi.org/10.1016/j.apergo.2022.103841.

Granzow, R.F., Schall, M.C., Smidt, M.F., Chen, H., Fethke, N.B., Huangfu, R., 2018. Characterizing exposure to physical risk factors among reforestation hand planters in the Southeastern United States. Appl. Ergon. 66, 1–8. https://doi.org/10.1016/j.apergo.2017.07.013.

Hansson, G., Asterland, P., Holmer, N. -g, Skerfving, S., 2001. Validity and reliability of triaxial accelerometers for inclinometry in posture analysis. Med. Biol. Eng. Comput. 39, 405–413. https://doi.org/10.1007/BF02345361.

Hansson, G.-Å., Arvidsson, I., Ohlsson, K., Nordander, C., Mathiassen, S.E., Skerfving, S., Balogh, I., 2006. Precision of measurements of physical workload during standardised manual handling. Part II: inclinometry of head, upper back, neck and upper arms. J. Electromyogr. Kinesiol. 16, 125–136. https://doi.org/10.1016/j.jelekin.2005.06.009.

Hibbing, P.R., Lamunion, S.R., Kaplan, A.S., Crouter, S.E., 2018. Estimating energy expenditure with ActiGraph GT9X inertial measurement unit. Med. Sci. Sports Exerc. 50, 1093–1102. https://doi.org/10.1249/mss.0000000000001532.

Johnson, G., Pianosi, P., Rajamani, R., 2022. Estimation of three-dimensional thoracoabdominal displacements during respiration using inertial measurement units. IEEE ASME Trans. Mechatron. 1–11. https://doi.org/10.1109/TMECH.2022.3151837.

Kersten, J.T., Fethke, N.B., 2019. Radio frequency identification to measure the duration of machine-paced assembly tasks: agreement with self-reported task duration and application in variance components analyses of upper arm postures and movements recorded over multiple days. Appl. Ergon. 75, 74–82. https://doi.org/10.1016/j.apergo.2018.09.005.

Ligorio, G., Sabatini, A.M., 2015. A linear Kalman Filtering-based approach for 3D orientation estimation from Magnetic/Inertial sensors. In: 2015 IEEE International Conference on Multisensor Fusion and Integration for Intelligent Systems (MFI). Presented at the 2015 IEEE International Conference on Multisensor Fusion and Integration for Intelligent Systems. MFI, pp. 77–82. https://doi.org/10.1109/MFI.2015.7295749.

Manivasagam, K., Yang, L., 2022. Evaluation of a new simplified inertial sensor method against electrogoniometer for measuring wrist motion in occupational studies. Sensors 22, 1690. https://doi.org/10.3390/s22041690.

Marcotte, R.T., Bassett, D.R., Weinhandl, J.T., Crouter, S.E., 2018. Application of the ActiGraph GT9X IMU for the assessment of turning during walking and running. Biomed. Phys. Eng. Express 4, 065003. https://doi.org/10.1088/2057-1976/aad0d0.

Pedley, M., 2013. Tilt Sensing Using a Three-Axis Accelerometer (Application Note No. AN3461).

Robert-Lachaine, X., Larue, C., Denis, D., Delisle, A., Mecheri, H., Corbeil, P., Plamondon, A., 2019. Feasibility of quantifying the physical exposure of materials handlers in the workplace with magnetic and inertial measurement units. Ergonomics 1–10. https://doi.org/10.1080/00140139.2019.1612941, 0.

Schall Jr., M.C., Fethke, N.B., Chen, H., 2016a. Working postures and physical activity among registered nurses. Appl. Ergon. 54, 243–250. https://doi.org/10.1016/j.apergo.2016.01.008.

Schall Jr., M.C., Fethke, N.B., Chen, H., Gerr, F., 2015. A comparison of instrumentation methods to estimate thoracolumbar motion in field-based occupational studies. Appl. Ergon. 48, 224–231. https://doi.org/10.1016/j.apergo.2014.12.005.

Schall Jr., M.C., Fethke, N.B., Chen, H., Oyama, S., Douphrate, D.I., 2016b. Accuracy and repeatability of an inertial measurement unit system for field-based occupational studies. Ergonomics 59, 591–602. https://doi.org/10.1080/00140139.2015.1079335.

Schall, M.C., Zhang, X., Chen, H., Gallagher, S., Fethke, N.B., 2021. Comparing upper arm and trunk kinematics between manufacturing workers performing predominantly cyclic and non-cyclic work tasks. Appl. Ergon. 93, 103356 https://doi.org/10.1016/j.apergo.2021.103356.

Veiersted, K.B., Gould, K.S., Østerås, N., Hansson, G.-Å., 2008. Effect of an intervention addressing working technique on the biomechanical load of the neck and shoulders among hairdressers. Appl. Ergon. 39, 183–190. https://doi.org/10.1016/j.apergo.2007.05.007.

Yang, L., Grooten, W.J.A., Forsman, M., 2017. An iPhone application for upper arm posture and movement measurements. Appl. Ergon. 65, 492–500. https://doi.org/10.1016/j.apergo.2017.02.012.